

CARS investigation of collisional shift of the hydrogen Q-branch transitions by water at high temperatures[†]

K. A. Vereschagin,^{a*} A. K. Vereschagin,^a V. V. Smirnov,^a O. M. Stel'makh,^a
V. I. Fabelinsky,^a W. Clauss^b and M. Oschwald^b

A high-resolution ($\sim 0.1 \text{ cm}^{-1}$) spectroscopic method based on the application of a Fabry–Pérot interferometer to the spectral analysis of the coherent anti-Stokes Raman scattering (CARS) signal from an individual Raman transition was used to obtain single-shot spectra of hydrogen Q-branch transitions directly in the flame of a pulsed, high-pressure H_2/O_2 combustion chamber. Simultaneously with the Fabry–Pérot pattern, a broadband CARS spectrum of the complete H_2 Q-branch structure was recorded in order to measure the temperature of the probe volume. During every cycle of the combustion chamber, a pressure pulse together with single-shot CARS spectra, providing information on individual line shapes and medium temperature, was recorded. On the basis of the experimental data, the temperature dependences of lineshift coefficients for several Q-branch lines of hydrogen molecules under collisions with water molecules were determined in the temperature range $2100 < T < 3500 \text{ K}$, and an empirical 'fitting law' for H_2 – H_2O lineshift coefficients is proposed. Copyright © 2010 John Wiley & Sons, Ltd.

Keywords: CARS spectroscopy; linewidth measurements; collisional shift; Fabry–Pérot interferometry

Introduction

Our research concerns line-shape spectroscopy of hydrogen Q-branch transitions in various binary mixtures. Since the lines are well separated, hydrogen molecules are a suitable object for the study of the influence of collisions on the spectral line's contour. At densities of a gas mixture above 1 amagat and temperatures higher than 300 K, the contour of a spectral line is modified by collisional broadening and shift, and these line shape changes are evidently observed in the spectra of molecular hydrogen.

In previous years, some efforts were made to study hydrogen lineshift, since the influence of collisions on the lineshift in hydrogen is large in comparison with many other species. Semiclassical and quantum calculations provide some estimates of lineshift coefficients for H_2 – H_2 and H_2 –He, whereas none is available for H_2 – H_2O collisions since accurate intermolecular potentials for H_2 – H_2O are presently not known. Experimentally,^[1] pure H_2 (up to 1000 K) and several mixtures (pure H_2 , H_2 –He, H_2 – N_2)^[2] have been investigated by means of inverse Raman spectroscopy (IRS) in a heatable static cell in the temperature range 300–1200 K with high spectral resolution and accuracy. These measurements allow modeling the lineshift coefficients as a function of temperature and J quantum number. Michaut *et al.*^[2] have revealed that, whatever the perturber (H_2 , He, Ne, Ar, Xe, N_2), the temperature dependence of the lineshift is proportional to $T^{1/2}$:

$$\delta(J, T) = A_J \sqrt{T} + B_J \quad (1)$$

At the same time, a study^[3] of collisional broadening for the H_2 – H_2O system was carried out in a heatable cell at temperatures up to 1800 K, also by means of IRS. In these experiments, the contours of several individual spectral lines were

recorded with high resolution, were precisely analyzed and the data on line broadening coefficients were presented^[3]; however, no data concerning the lineshift coefficients were published. Also Chaussard *et al.*^[3] noted that the high chemical activity of water vapor at elevated temperatures and design constraints of the heatable cell restrict the opportunity to move to higher temperatures ($> 1800 \text{ K}$) in cell experiments.

To fill up the gap in information concerning collisional lineshift for H_2 – H_2O mixtures, especially at high temperatures, we undertook the present study. Our work has been devoted to a study of collisional broadening^[4,5] and shift of the Q-branch ($J = 1, 3, 5, 7, 9$) lines of hydrogen molecules in mixtures with water molecules at high temperatures ($2100 < T < 3500 \text{ K}$) by coherent anti-Stokes Raman scattering (CARS) spectroscopy. In this paper, we present the results obtained for the lineshifts.

To move into higher temperatures ($> 1800 \text{ K}$) and to avoid problems with the chemical activity of heated water, we decided to carry out our measurements directly in a H_2/O_2 combustion chamber with controllable and reproducible parameters. The flame of the H_2/O_2 high-pressure pulsed combustion chamber (HPPCC) is characterized by high gas temperatures (up to 3500 K) and pressures (up to 150 bar) with the following combustion product mix: H_2 , H_2O (major species) and atoms and radicals

* Correspondence to: K. A. Vereschagin, General Physics Institute, Vavilov Str. 38, 119991 Moscow, Russia. E-mail: veresch@kapella.gpi.ru

[†] Paper published as part of the ECONOS special issue.

^a General Physics Institute, Vavilov Str. 38, 119991 Moscow, Russia

^b German Aerospace Center, Space Propulsion Institute, Langer Grund, 74239 Hardthausen, Germany

(minor species). The gas parameters can fluctuate from shot to shot, so the single-shot mode is preferable for diagnostics.

For our measurements, we used the CARS technique (frequency domain, pulse duration ~ 10 ns). While the resolution of CARS itself allows the measurement of line-shape parameters, the CARS spectral shape depends both on the imaginary and real parts of the resonant nonlinear susceptibility, together with a nonresonant background contribution, making the analysis of the line shape quite complicated. IRS could provide very accurate measurements of linewidths and lineshifts; however, it is not suitable for measurements in the single-shot mode. Hence, in order to reach our goal, there was no alternative to CARS spectroscopy.

Measurements of gas parameters (temperature, pressure) and contour parameters (width, position) were made directly in the flame, at various densities and temperatures of combustion products, and at certain delays of CARS probe relative to flame ignition. As a result, temperature dependences of water-broadening and shift coefficients for several Q-branch hydrogen lines ($J = 1, 3, 5, 7, 9$) were obtained in the temperature range 2100–3500 K.

Experimental

The three-channel (see below) setup and the pulsed chamber are described in detail elsewhere.^[4–6] The combustion process was repetitive with a rate of 1 Hz. Each time after the H_2 – O_2 mixture had burned out, the outflow of the gas from the combustion chamber led to a drop in the pressure and temperature. This, in turn, allowed obtaining the data at various temperatures and pressures by varying the delay between the CARS probe and the ignition.

Pressure measurements were carried out by a high-speed piezoelectric pressure gauge Kistler 6061B, built into the wall of the combustion chamber (first channel).

Temperature measurements in the combustion chamber were carried out with the help of a broadband CARS spectrometer, which allowed registering a significant fragment of the hydrogen Q-branch spectrum during a single laser shot (second channel). A Jobin-Yvon THR-1000 grating spectrograph with a slit width of $\sim 1.5\text{ cm}^{-1}$ performed spectral analysis of the CARS signal in this second channel. The CARS spectrum was detected by a multichannel CCD detector.

High-resolution, single-shot spectra of a selected H_2 Q-branch line were measured simultaneously by another CARS spectrometer also during a single laser shot (third channel). Spectral analysis of the CARS signal in this third channel was carried out by a LOMO IT-28-30 Fabry–Pérot interferometer having a free spectral range of 1.66 cm^{-1} and a slit function width of $\sim 0.09\text{ cm}^{-1}$. Five series of measurements with ignition–CARS probe delays of 100, 200, 300, 400 and 600 μs were carried out for each of the spectral lines Q_1 , Q_3 , Q_5 , Q_7 and Q_9 . Each series consisted of 50 cycles (shots) of the pulsed burner.

All measurements were carried out during the burning of the fuel-rich hydrogen–oxygen mixtures (equivalence ratio $\Phi \sim 2$ –2.4), resulting (depending on the delay) in combustion product pressures of 30–80 bar, water vapor contents at the level of 30–50% and temperatures in the range of 2100–3500 K.

Results and Discussion

Gas parameters control

Procedures for gas temperature evaluation, density measurements and determination of the concentration of combustion products

are described elsewhere.^[4] Briefly, the broadband CARS spectra were processed, and temperature values for every cycle were obtained. Fast pressure gauge response, specific for temporal structure of a pressure pulse in each cycle of the combustion chamber, allowed determining gas density at any moment of the cycle by simultaneously measuring the temperature. The product composition was calculated by means of the GasEq program^[7] with the use of the measured values of temperature and pressure.

Line positions' measurements

Fabry–Pérot interferometer interference rings were detected by a two-dimensional CCD array. A specially developed software package made angular integration of a circular fringe structure (to minimize the influence of noise), normalized the interference patterns on the light intensity distribution over a cross-section of a CARS beam and realized a fitting procedure of the experimental interferogram by a convolution of the Airy function (interferometer slit function) with the Lorentzian contour (spectral line profile). A fitting procedure with four fitting parameters (baseline, scaling factor, linewidth and central wavelength) provided the line position Ω_0 and the spectral line contour width Γ .

As an example, the line-shape parameters for the Q_7 line *versus* delay and density are shown in Fig. 1, and one can see that the changes of the measured values obey some regular dependence. Note that every point of the graph corresponds to a different time delay with its unique temperature value and, hence, the line-shape parameters should not depend linearly on density.

Let us also remember that the resonant and nonresonant terms contribute to a third-order nonlinear susceptibility $\chi^{(3)}$:

$$\chi^{(3)} = \chi_R^{(3)} + \chi_{NR}^{(3)} \quad (2)$$

The nonresonant contribution originates from the movement of electrons of a molecule in the electrical field of the interacting light waves; it is a real quantity and practically does not depend on frequency, but is linearly dependent on the density of molecules. On the contrary, the resonant contribution originates from the movement of nuclei in the electrical field of the light waves and has a pronounced dependence on frequency, gas density N and temperature T . In the simple case of ro-vibrational branch without a spectral exchange, $\chi_R^{(3)}$ can be expressed^[8] as a sum of a set of terms, where each term represents the contribution from an individual transition. Resonant nonlinear susceptibility is a complex quantity, and its real and imaginary parts differently depend on the detuning from a resonance (Ω_J , γ_J). For homogeneously broadened transitions, the imaginary part at large detuning ($[\Omega_J - (\omega_1 - \omega_2)] \gg \Gamma_J$) drops much faster than the real part, and it means that the neighboring transitions can contribute to the value of the real part of the susceptibility of the transition examined, whereas contributions to the imaginary part can be neglected. Hence, the contribution from the wings of the real parts of a resonant susceptibility $\text{Re}[(\chi_R^{(3)})_i]$ ($i \neq J$) of the neighboring ro-vibrational transitions can be regarded as a real quantity which is constant on the scale of the linewidth Γ_J but is varying from line to line. The low-frequency wing from the real part of the resonant susceptibility of the water Q-branch also contributes very much to this quantity. Together with weakly varying electronic nonresonant susceptibility χ_{NR}^{el} it forms an 'effective'^[9] nonresonant background at the location of

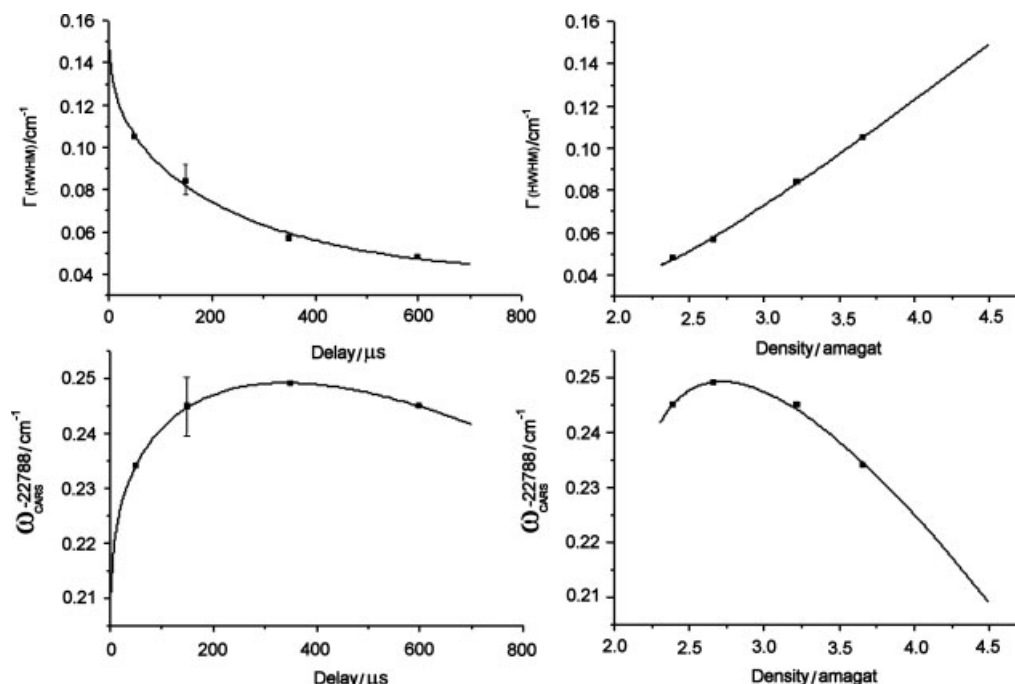


Figure 1. Line-shape parameters for hydrogen Q₇ line *versus* density. Smooth curves are supporting lines (a polynomial of the second order relative to $T^{1/2}$) showing that changes of measured values are natural and quite regular.

the transition with rotational quantum number J :

$$(\chi_{NR}^{(3)})_J^{\text{eff}} = \sum_{i \neq J} \text{Re}(\chi_i^{(3)})_R + \text{Re}(\chi_{H_2O}^{(3)})_R + \chi_{NR}^{\text{el}} \quad (3)$$

The nonresonant contribution to the third-order nonlinear susceptibility $\chi^{(3)}$ specifically disturbs the line shape of an individual Raman transition (Fig. 2). Because of the specific CARS line shape resulting from the interference with the nonresonant background, an additional CARS lineshift arises. This additional shift ('CARS shift', Δ_{CARS}) depends on nonresonant background value, linewidth and slit function of the spectrometer. The CARS shift of the Q-branch lines can be considered as the CARS shift of the isolated lines in the presence of an 'effective' nonresonant background.

For calculation of the shift coefficients, we have corrected each of the obtained line position Ω_0 for the CARS shift. The magnitude and sign of the 'effective' nonresonant background were determined from BB-CARS spectra processing (second channel), and transition linewidths [obtained^[4] together with line positions from the 'fitting' procedure (third channel)] as well as the Fabry–Pérot interferometer slit function were taken into account during CARS shift calculations. Stark shift was neglected for all the lines since it was rather small compared to CARS shift and collisional self-shift.

Collisional lineshift coefficients and their temperature dependences

When processing the experimental data, we assumed that collisional lineshift linearly depends on the density, and the

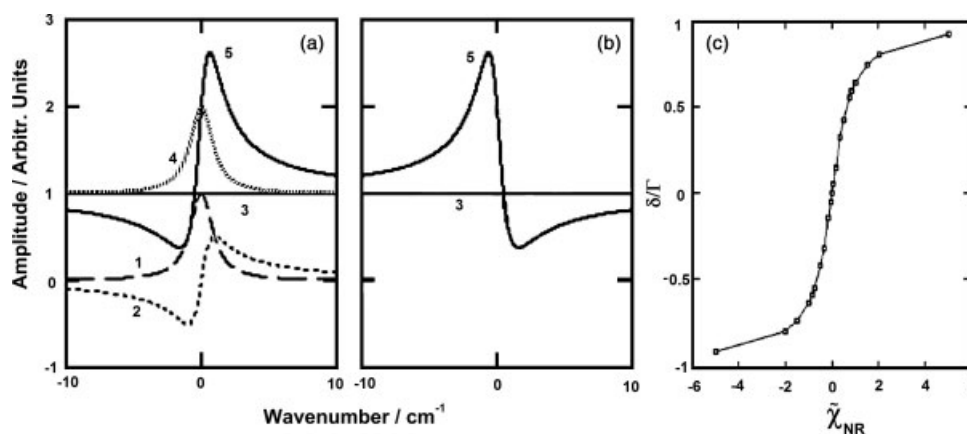


Figure 2. CARS line profile (a and b) for Lorentzian spectrum and reduced shift (c) of maximum of CARS profile *versus* nonresonant background χ_{NR} (ratio of 'nonresonant' to maximum 'resonant' susceptibilities). (1) $\text{Im}(\chi_R^{(3)})$; (2) $\text{Re}(\chi_R^{(3)})$; (3) $|\chi_{NR}^{(3)}|^2$; (4) $\{[\text{Im}(\chi_R^{(3)})]^2 + |\chi_{NR}^{(3)}|^2\}$; (5) CARS spectral profile. (a) $\chi_{NR} > 0$ and (b) $\chi_{NR} < 0$, $\Gamma = 1 \text{ cm}^{-1}$, $\chi_{NR} = 1$. With the use of any device for spectral analysis, the reduced shifts (δ/Γ) become dependent on the slit function of the spectrometer.

positions $\Omega(T, \rho)$ of the observed lines were defined on the basis of the expression:

$$\Omega(T, \rho) = \Omega_0 + \delta(T)\rho + \Delta_{\text{CARS}} \quad (4)$$

where Ω_0 is the anti-Stokes frequency at zero density, ρ is the density (total) of a gas mixture in amagat units, $\delta(T)$ is the collisional lineshift coefficient for a binary H_2 – H_2O mixture at a given H_2 concentration and Δ_{CARS} stands for the CARS shift. After the correction on the CARS shift, the collisional lineshift coefficients are defined as

$$\delta(T) = \frac{\Omega(T, \rho) - \Omega_0}{\rho} \quad (5)$$

Usually, collisional lineshift coefficients in binary mixtures obey a so-called linear mixing rule.^[2] For mixtures of hydrogen with nitrogen and with a number of noble gases, this rule is broken, but for H_2 – H_2 and H_2 – H_2O mixtures the linear law is valid,^[2,3] and

$$\delta(\text{CH}_2, \text{CH}_2\text{O}) = \delta_{\text{H}_2-\text{H}_2}\text{CH}_2 + \delta_{\text{H}_2-\text{H}_2\text{O}}\text{CH}_2\text{O} \quad (6)$$

Thus, the lineshift coefficients (Eqn (5)) should be interpreted according to Eqn (6), and for the lineshift coefficients of the hydrogen Q-branch lines due to collisions with water molecules one gets

$$\delta_{\text{H}_2-\text{H}_2\text{O}} = \frac{\delta(\text{CH}_2, \text{CH}_2\text{O}) - \delta_{\text{H}_2-\text{H}_2}\text{CH}_2}{\text{CH}_2\text{O}} \quad (7)$$

As follows from Eqn (7), the hydrogen–water lineshift coefficients are obtained from experimentally measured ‘full’ ones $\delta(\text{CH}_2, \text{CH}_2\text{O})$ by subtraction of self-broadening contribution. Although we supposed that the dominant contribution to the measured lineshift coefficients is determined by collisions with water molecules, nevertheless we took the self-shifting contribution into account by extrapolating the data^[1,2] for pure H_2 .

Reproducibility of our results is illustrated by Fig. 3. There exist two datasets for Q_7 shift coefficients corresponding to two test runs with different initial pressures of the HPPCC. Both datasets fit with the same straight line, corresponding to a linear dependence of shift coefficients on $T^{1/2}$.

The results of the measurements for hydrogen Q-branch lines Q_1 , Q_3 , Q_5 , Q_7 and Q_9 obtained in the present work are shown in Fig. 4. We accept that the temperature dependence of shift

coefficients is described by Eqn (1). On the top part of Fig. 4, the results of the fitted linear dependencies of the shift coefficients on $T^{1/2}$ are presented as straight lines. Below (Fig. 4), the coefficients A_J and B_J from Eqn (1) are plotted *versus* the rotational quantum number J . We found that the following power law gives a very satisfactory representation of coefficients A_J and B_J (Fig. 4):

$$A_J = [a_0 + a_1\sqrt{J} + a_2J]^{-1}, B_J = [b_0 + b_1\sqrt{J} + b_2J]^{-1} \quad (8)$$

With the determination of the coefficients A_J and B_J , one can, as has been done in Ref. [2] for H_2 – X ($\text{X} = \text{H}_2$, He , N_2) mixtures, introduce an empirical ‘fitting law’ for H_2 – H_2O lineshift coefficients:

$$\delta(J, T) = \frac{\sqrt{T}}{a_0 + a_1\sqrt{J} + a_2J} + \frac{1}{b_0 + b_1\sqrt{J} + b_2J} \quad (9)$$

In Ref. [2], it was found that the different straight lines given by Eqn (1) seem to intersect at a unique point for different J values, when extrapolated to low temperatures. The existence of such a crossing point was interpreted as the beginning of the J -dependence at some temperature T_0 ; the value of lineshift coefficient at T_0 would correspond to the usual J -independent vibrational shift. At the same time, the shift coefficients for pure H_2 do not manifest any unique crossing point of the straight lines corresponding to different J values. Michaut *et al.*^[2] have supposed that in pure H_2 there was an additional contribution to the J -dependent collisional shift: a coupling shift.^[10] After removing the calculated coupling shift contribution from the experimental shift, they have obtained a typical crossing point of all the straight lines of Eqn (1) for all the J 's.

Unlike in the earlier work,^[2] the curves given by Eqn (9) do not intersect in a unique point when extrapolated to low temperatures. Since the J -independent vibrational shift should still exist, it could mean that another (unknown) additional contribution to the J -dependent collisional shift exists.

To summarize, we can emphasize the four main properties of our results: (1) The measured H_2 – H_2O lineshift coefficients prove to be both positive and negative – depending on J -value and temperature; (2) The derivatives with respect to temperature of the shift coefficients are negative for all the J values: H_2 – H_2O shift coefficients decrease with temperature increase; (3) The measured absolute values of the H_2 – H_2O shift coefficients are by the order of magnitude comparable with H_2 – X ($\text{X} = \text{H}_2$, He , N_2) coefficients; (4) A linear extrapolation of the H_2 – H_2O shift coefficients with $T^{1/2}$ to lower temperatures gives values that are significantly larger than that of H_2 – X coefficients.

The magnitudes of the shift coefficients do not follow a smooth dependence on J . Any ‘ready’ explanation for such a non-monotonic behavior of the shift coefficients is presently not available in the literature and, perhaps, it poses a challenge for a future work.

The presented results can be used both in experimental and theoretical researches. As is well known, the CARS spectra of hydrogen Q-branch transitions are used for combustion thermometry of hydrogen-containing mixtures. In order to derive accurate information about the temperature and species concentration from CARS spectroscopy, one needs to know the nonlinear susceptibility of the sample, and the information about the position and width of every line of the spectrum over a wide temperature range (1000–3500 K) is very important. Our results allow reproduction of the behavior of the collisional shift *versus* temperature at the

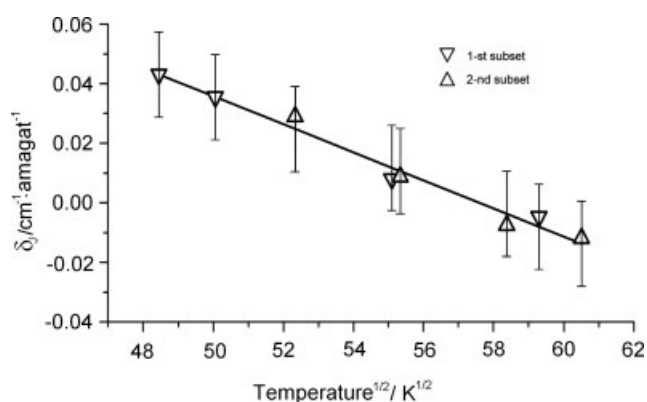


Figure 3. Collisional H_2 – H_2O shift coefficients *versus* $T^{1/2}$ for Q_7 line. Two datasets correspond to different test runs. Error bars show a typical measurement error related to data for all H_2 Q-branch lines investigated.

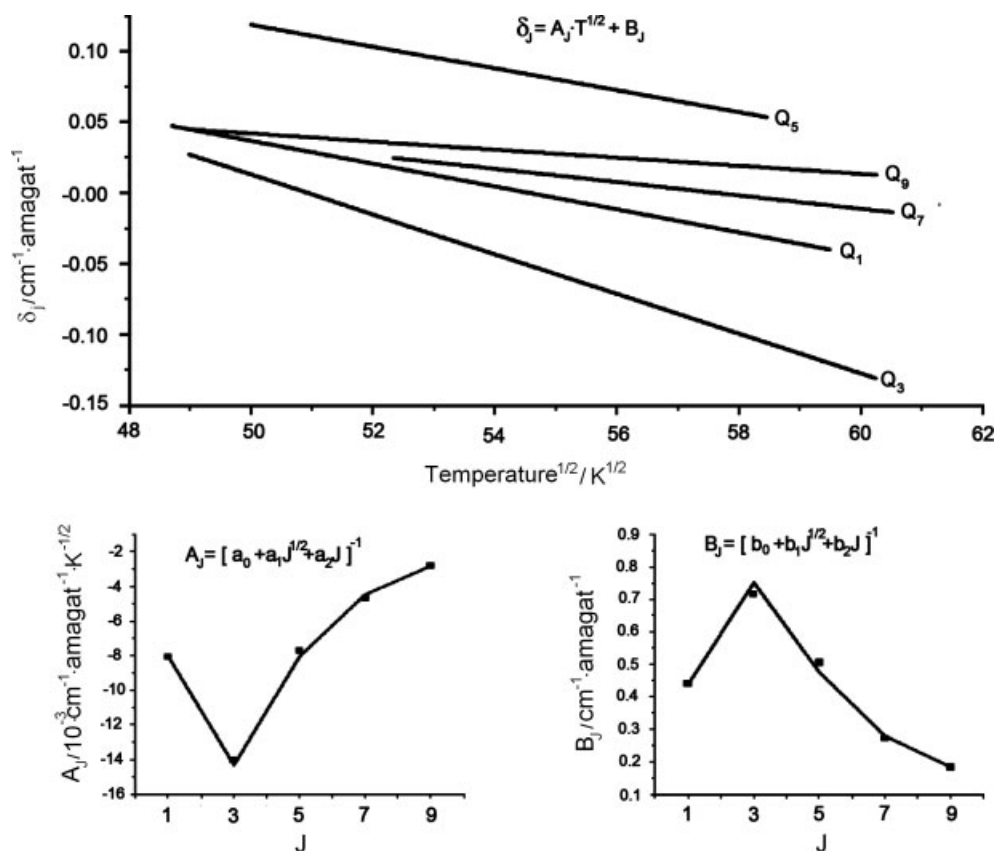


Figure 4. Top: the results presented as straight lines of fitted linear dependence of shift coefficients on $T^{1/2}$. Bottom: coefficients A_J and B_J from Eqn (1) plotted versus rotational quantum number J ; the curves interpolating A_J and B_J represent functions of the type $(a_0 + a_1 J^{1/2} + a_2 J)^{-1}$.

above-mentioned conditions for rotational states $J = 1, 3, 5, 7, 9$. From a more fundamental point of view, accurate measurements of Raman line-shape parameters can provide valuable information on the intermolecular potentials – the basis for creation of adequate models describing the shape of spectral lines. Perhaps, comparison of data for $\text{H}_2\text{-X}$ ($\text{X} = \text{H}_2, \text{He}, \text{Ne}, \text{Ar}, \text{Xe}, \text{N}_2$) pairs with our results would be of interest to clarify the effect of the ‘nonpolar–polar’ molecular interaction on collisional shift.

Conclusions

In the present work, lineshift coefficients for hydrogen Q-branch lines due to collisions with water molecules at temperatures from 2100 to 3500 K were measured. To achieve these high temperatures, measurements were carried out inside a high-pressure pulsed hydrogen–oxygen combustion chamber. The use of a real flame is, probably, the only way to move up to elevated (>2000 K) temperatures for studying collisional broadening and shift. The high pressure pulsed combustion chamber (HPPCC) can become a good laboratory device for such researches; however, its application demands either high operational stability of the HPPCC (then it is possible to apply SRS techniques) or the ability to work in single-shot CARS. CARS is not the best way for fine researches on the spectral features of a line contour; however, probably, there hardly exist any alternatives if it is necessary to perform the measurements in a nonstationary system like the flame of an HPPCC. Consideration of additional line shift due to interference with the nonresonant background allows allocating

the contribution from J -dependent collisional shift in the total change of transition frequency.

Acknowledgement

The authors gratefully acknowledge financial support for part of this work by INTAS (project no. INTAS 05-1000008-7951. Field 6).

References

- [1] L. A. Rahn, G. J. Rosasco, *Phys. Rev.* **1990**, *41*, 3698.
- [2] J. X. Michaut, J.-P. Berger, P. M. Sinclair, H. Berger, *J. Quant. Spectrosc. Radiat. Transfer* **1998**, *60*(4), 585.
- [3] F. Chaussard, X. Michaut, R. Saint-Loup, H. Berger, P. Joubert, J. Bonamy, D. Robert, *Poster presentation at ECONOS Villigen (Switzerland)*, 18–19 March, **2002**.
- [4] K. A. Vereschagin, A. K. Vereschagin, V. V. Smirnov, O. M. Stelmakh, V. I. Fabelinsky, W. Clauss, M. Oswald, *J. Raman Spectrosc.* **2008**, *39*, 722.
- [5] W. Clauss, D. N. Klimenko, M. Oswald, K. A. Vereschagin, V. V. Smirnov, O. M. Stelmakh, V. I. Fabelinsky, *J. Raman Spectrosc.* **2002**, *33*, 906.
- [6] K. A. Vereschagin, V. V. Smirnov, O. M. Stelmakh, V. I. Fabelinsky, W. Clauss, D. N. Klimenko, M. Oswald, A. K. Vereschagin, *J. Raman Spectrosc.* **2005**, *36*, 134.
- [7] C. Morley, <http://www.gaseq.co.uk> [accessed 2010].
- [8] J. C. Luthe, E. J. Beiting, F. Y. Yueh, *Comput. Phys. Commun.* **1986**, *42*, 73.
- [9] K. A. Vereschagin, V. V. Smirnov, *Proceedings of SPIE* **2001**, *4429*, 128.
- [10] A. D. May G. Varghese, J. C. Stryland, H. L. Welsh, *Can. J. Phys.* **1964**, *42*, 1058.